Journal of Alloys and Compounds 504 (2010) 181–185

Contents lists available at ScienceDirect

Journal of Alloys and Compounds

journal homepage: www.elsevier.com/locate/jallcom

Isothermal section at 1100 °C of the Fe–Ni–Ta system

Chengying Tang[a,b,*], Minmin Tong[a], Honghui Xu[b], Yong Du[b], Joonho Lee[c], Qingrong Yao[a], Yuehui He[b], Huaiying Zhou[a]

[a] Department of Materials Science and Engineering, Guilin University of Electronic Technology, Guilin, Guangxi 541004, PR China
[b] State Key Laboratory of Powder Metallurgy, Central South University, Changsha, Hunan 410083, PR China
[c] Department of Materials Science and Engineering, Korea University, 5-1 Anam-dong, Seongbuk-gu, Seoul 136-713, Republic of Korea

ARTICLE INFO

Article history:
Received 28 February 2010
Received in revised form 11 May 2010
Accepted 21 May 2010
Available online 27 May 2010

Keywords:
Ternary alloy systems
Diffusion
Phase diagrams
Scanning electron microscopy
Electron microprobe

ABSTRACT

The isothermal section of the Fe–Ni–Ta system at 1100 °C was constructed using 6 diffusion couples and 10 alloys, the compositions of which were selected on the basis of the experimental results of the (Fe–Ni alloy)/Ta diffusion couples. The samples were examined by means of optical microscopy, scanning electron microscopy, and electron probe microanalysis. Experimental results showed no existence of ternary compounds at 1100 °C. The following five three-phase equilibria were observed: (1) (Ta) + Ta_2Ni + Ta(Fe, Ni), (2) Fe_2Ta + Ta (Fe, Ni) + $TaNi_2$, (3) Fe_2Ta + $TaNi_2$ + $TaNi_3$, (4) Fe_2Ta + $TaNi_3$ + (Fe, Ni), (5) $TaNi_3$ + $TaNi_8$ + (Fe, Ni). The compounds FeTa and NiTa formed continuous solid solution. The solubility of Fe in $TaNi_2$ and $TaNi_3$ was determined to be 18 and 7.8 at.%, respectively, while the solubility of Ni in Fe_2Ta was estimated to be 40 at.%.

1. Introduction

Bulk metallic glasses (BMG) had received a great deal of attention due to the scientific and technological interest in the past decades [1]. A large number of novel amorphous alloy systems based on various elements had been developed recently [2–8]. Many studies on the glass transition and crystallization process, glass forming ability (GFA) and the correlation between the GFA and the thermodynamics of glassy alloys had been conducted extensively [9–14]. Fe–Ni–Ta system had received attention because it was relevant for the amorphous, magnetic head, and corrosion-resistant steel materials [15–22]. Knowledge of the phase relationships of the Fe–Ni–Ta system was the basis of the thermodynamics and of interest for the development of these materials. Gupta [23] measured a partial isothermal section at 1340 °C (Ta < 15 at.%) of the Fe–Ni–Ta system, who only determined the solubility of Ta in (Fe, Ni) with no determined three-phase equilibrium. Uskova [24] determined an isothermal section at 1000 °C of the Fe–Ni–Ta system using equilibrated alloys. It was experimentally indicated that the diffusion couple technique, supplemented with equilibrated ternary alloys was a high-efficiency approach for the phase diagram determination [25–30]. The objective of the present work was to investigate the phase equilibria of the Fe–Ni–Ta system at 1100 °C using this high-efficiency approach.

Among the Fe–Ni–Ta system, the Fe–Ta system was thermodynamically evaluated by Swartzendruber and Paul [31], and Okamoto [32], and the latest assessment was carried out by Srikanth and Petric [33]. There were two intermediate phases in this system, i.e., the μ phase FeTa, and the ε phase Fe_2Ta with a Laves structure. Ansara and Selleby [34], Cui and Jin [35] performed a thermodynamic assessment of the Ni–Ta system. There were five intermediate phases in the Ni–Ta system, viz. Ta_2Ni, TaNi, $TaNi_2$, $TaNi_3$ and $TaNi_8$. At low temperature ($\leq$550 °C) there was an ordered $FeNi_3$ phase with $L1_2$ structure in the Fe–Ni system [36].

2. Experimental

Fe (99.9 wt.% purity) and Ni (99.9 wt.%), and Ta (99.99 wt.%) were used as the starting materials. Six Fe–Ni binary alloys, the nominal compositions of which were listed in Table 1, were prepared by arc-melting pure elements in an arc furnace (WKDHL-1, Opt-electronics Co. Ltd., Beijing, China) under argon atmosphere using a non-consumable tungsten electrode. The ingots were re-melted six times to improve their homogeneity. Slices of approximate dimensions of 4 mm × 4 mm × 12 mm were cut from the ingots. Six different (Fe–Ni alloy)/Ta diffusion couples of 8 mm × 8 mm × 12 mm, were made of the elemental Ta and the Fe–Ni alloys. The method of preparing the specimens was described in [25–27]. The well–prepared (Fe–Ni alloy)/Ta diffusion couples were sealed in a silicon capsule back-filled with high purity argon, and annealed in an L4514-type diffusion furnace (Qingdao Instrument & Equipment Co. Ltd., China) at 1100 ± 2 °C for 600 h and then quenched into cold water.

After standard metallographic preparation, the microstructures of the Fe–Ni–Ta diffusion couples were first examined by means of optical microscopy (Leica DMLP, Germany), and scanning electron microscopy (SEM) (JSM-5600LV, JEOL, Japan). The

* Corresponding author at: Department of Materials Science and Engineering, Guilin University of Electronic Technology, 1 Jinji Road, Guilin, Guangxi 541004, PR China. Tel.: +86 130 77653978; fax: +86 773 2191903.
E-mail addresses: ctang@guet.edu.cn, csutcy@163.com (C. Tang).

0925-8388/$ – see front matter © 2010 Elsevier B.V. All rights reserved.
doi:10.1016/j.jallcom.2010.05.084

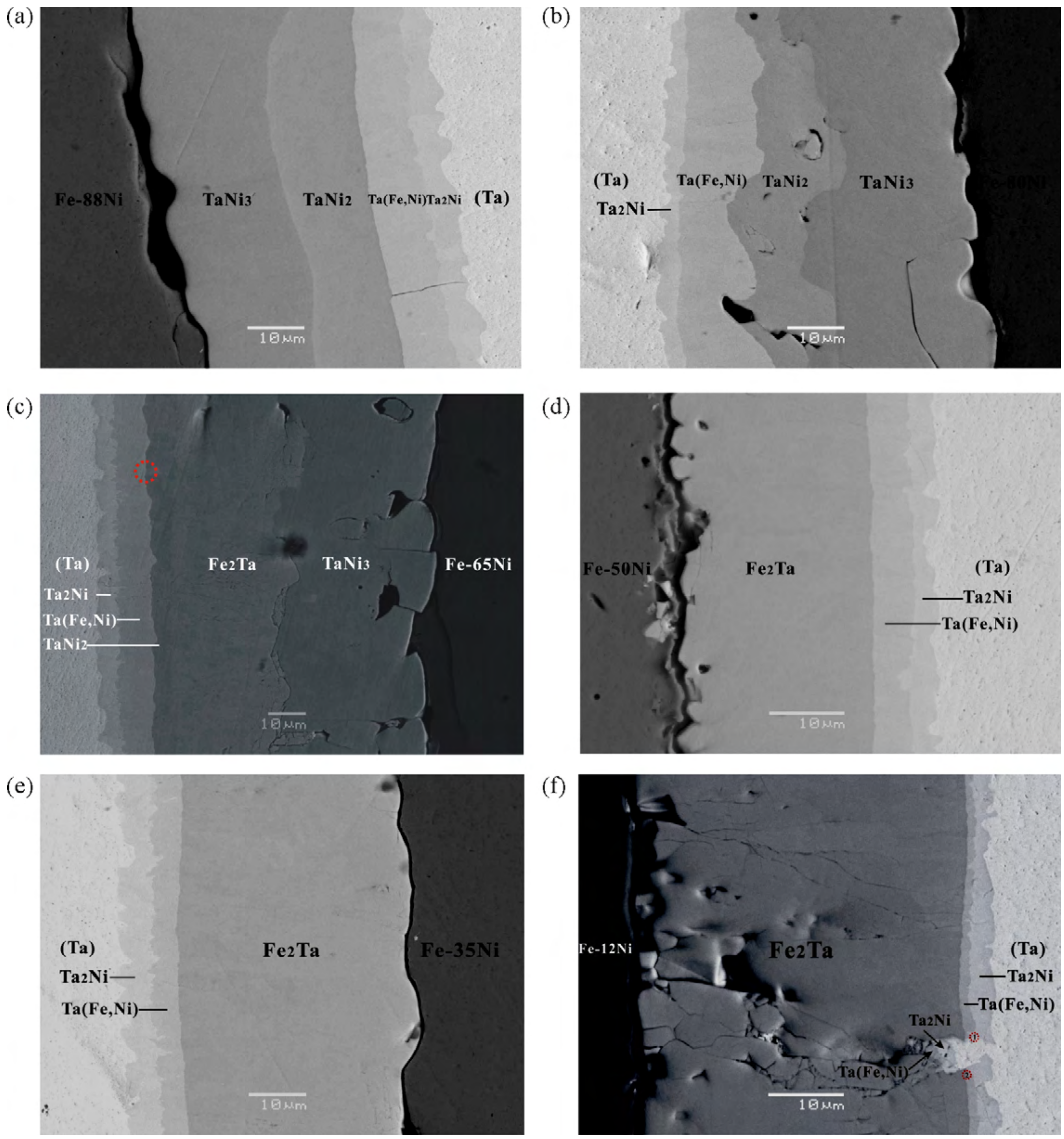

Fig. 1. Backscattered electron images of the (Fe–Ni alloy)/Ta diffusion couples annealed at 1100 °C for 600 h (a) (Fe–88Ni)/Ta; (b) (Fe–80Ni)/Ta; (c) (Fe–65Ni)/Ta; (d) (Fe–50Ni)/Ta; (e) (Fe–35Ni)/Ta; (f) (Fe–12Ni)/Ta.

phase equilibrium data in the diffusion couple were determined by energy dispersive X-ray (EDX) and electron probe microanalysis (EPMA) (JXA-8800R, JEOL, Japan). The results of EPMA were given after calibration with pure Fe, Ni, and Ta. The composition–distance curves for each element were determined using EPMA. The microprobe measurements were performed perpendicular to the interfaces between every two adjacent phases in the diffusion couples. The equilibrium compositions of each phase were obtained by extrapolating the composition–distance curves for each element to the phase boundaries.

Subsequently, 10 Fe–Ni–Ta ternary alloys listed in Table 2 were selected on the basis of the above experimental results obtained with EDX/EPMA measurement of the diffusion couples to substantiate some of the phase equilibria of the Fe–Ni–Ta system. The alloys prepared by arc melting were annealed at 1100 °C for 300 h and then water-quenched. The annealed alloy samples were then performed X-ray diffraction (XRD) analysis, and examined using SEM/EDX and EPMA.

3. Results and discussion

The microstructures of six (Fe–Ni alloy)/Ta diffusion couples annealed at 1100 °C for 600 h were shown in Fig. 1, respectively. The backscattered electron images of four representative Fe–Ni–Ta alloys annealed at 1100 °C for 300 h were presented in Fig. 2. A typical example for the concentration profiles of Fe, Ni and Ta in (Fe–65Ni)/Ta diffusion couple was given in Fig. 3.

Table 1
The nominal compositions of six Fe–Ni binary alloys used to prepare (Fe–Ni alloy)/Ta diffusion couples (in at.%).

	Alloy no.					
	1	2	3	4	5	6
Fe	12	20	35	50	65	88
Ni	88	80	65	50	35	12

Table 2
Nominal compositions of 10 Fe–Ni–Ta ternary alloys (in at.%).

	No.									
	1	2	3	4	5	6	7	8	9	10
Fe	19	30	35	46	48	25	3	5	6	14
Ni	16	10	5	11	6	55	86	84	64	48
Ta	65	60	60	43	46	20	11	11	30	38

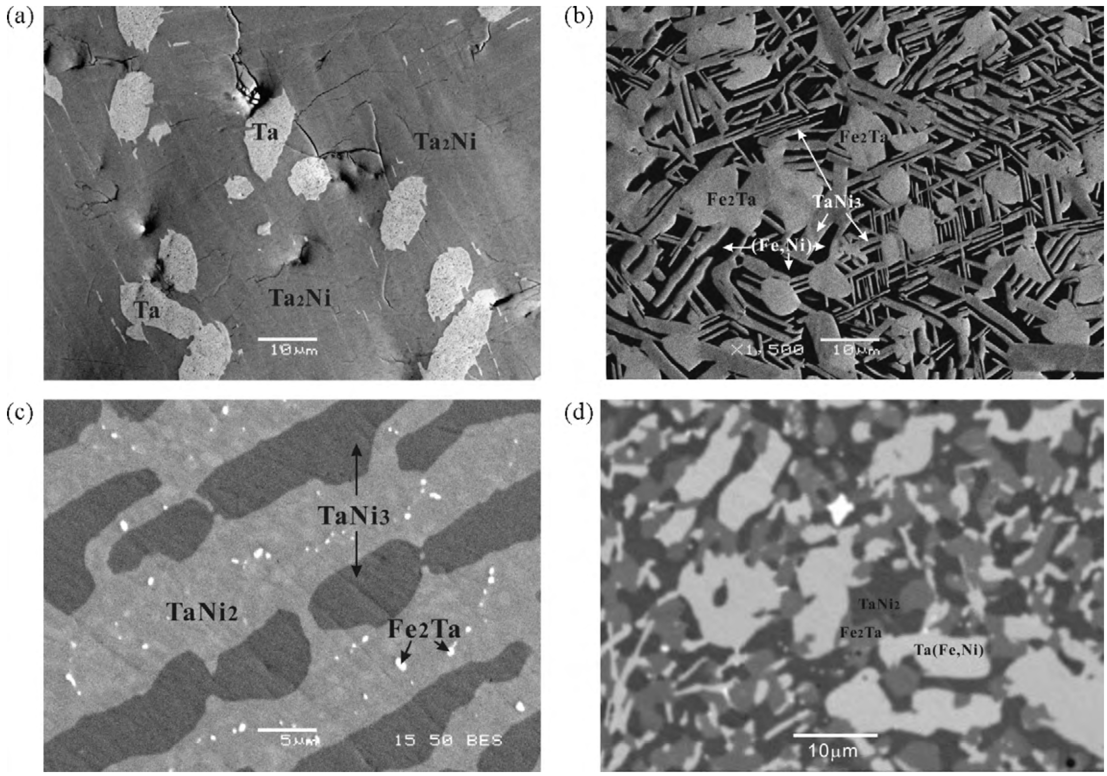

Fig. 2. Backscattered electron images of four representative alloys annealed at 1100 °C for 300 h; (a) Alloy 1 ($Fe_{19}Ni_{16}Ta_{65}$); (b) Alloy 6 ($Fe_{25}Ni_{55}Ta_{20}$); (c) Alloy 9 ($Fe_6Ni_{64}Ta_{30}$); (d) Alloy 10 ($Fe_{30}Ni_{10}Ta_{60}$).

As shown in Fig. 1, after inter-diffusion at 1100 °C for 600 h, several different phases with different thickness were formed in the six diffusion couples, respectively. The sequences of the phases formed in the diffusion couples 1 (Fe–88Ni)/Ta and 2 (Fe–80Ni)/Ta were the same, which indicated the same diffusion paths in diffusion couples 1 and 2, viz. (Ta) → Ta_2Ni → Ta(Fe, Ni) → $TaNi_2$ → $TaNi_3$ → (Fe, Ni). The sequence of the phases, indicating the difffusion path, in the diffusion couple 3 (Fe–65Ni)/Ta was (Ta) → Ta_2Ni → Ta(Fe, Ni) → Ta_2Ni → Fe_2Ta → $TaNi_3$ → (Fe, Ni). The sequences of the phases in the remaining three diffusion couples 4–6, (Fe–50Ni)/Ta, (Fe–35Ni)/Ta and (Fe–12Ni)/Ta, were the same, viz. (Ta) → Ta_2Ni → Ta(Fe, Ni) → Fe_2Ta → (Fe, Ni), which suggested the same diffusion paths in these three diffusion couples.

Additionally, the microstructure observation of the diffusion couple 3 (Fe–65Ni)/Ta (Fig. 1c) showed that the phases Ta(Fe, Ni), $TaNi_2$ and Fe_2Ta were in a three-phase equilibrium (marked with a dashed circle), which was substantiated by the microstructure of the diffusion couple 6 (Fe–12Ni)/Ta (marked with dotted circle 2) and Alloy 10 ($Fe_{14}Ni_{48}Ta_{38}$), as shown in Figs. 1f and 2d. It was found that the (Ta), Ta_2Ni and Ta(Fe, Ni) were in a three-phase equilibrium from the microstructure of diffusion couple 6 (Fe–12Ni)/Ta, as marked with dashed circle 1 of Fig. 1f. In the present work, the three-phase equilibria, Fe_2Ta, $TaNi_2$, $TaNi_3$, and $TaNi_8$ (Fe, Ni), $TaNi_3$, were not well determined, and presented in dashed lines in Fig. 4, because the size of the dot-shaped Fe_2Ta phase was too

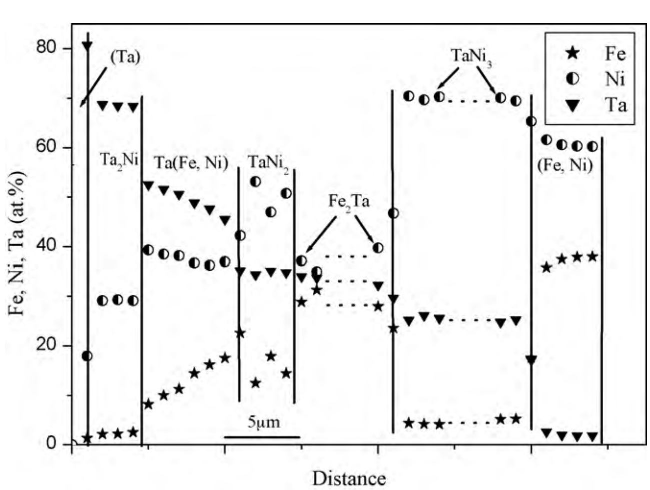

Fig. 3. Concentration profiles of Fe, Ni, and Ta in the diffusion couple 3 (Fe–65Ni)/Ta.

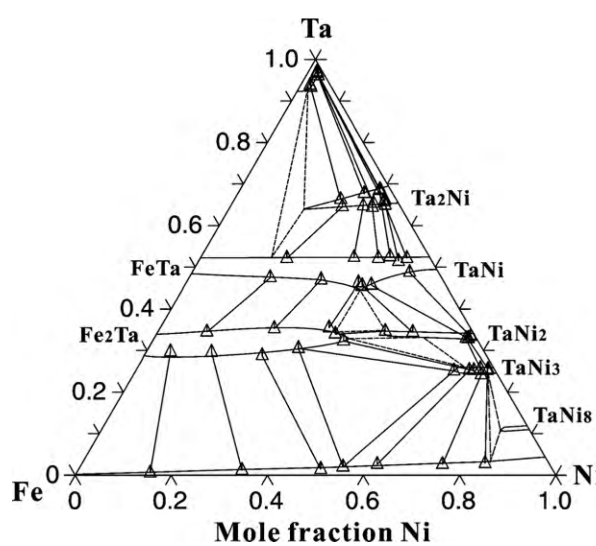

Fig. 4. Isothermal section at 1100 °C of the Fe–Ni–Ta system according to the present work.

Table 3
The tie-line data on the phase equilibria of the Fe–Ni–Ta system at 1100 °C (in at.%).

(Ta)			Ta_2Ni			Remarks[a]
Fe	Ni	Ta	Fe	Ni	Ta	
1.2	1.8	97.0	1.8	33.1	65.1	DC 1
1.3	2.0	96.7	2.4	31.4	66.2	DC 2
1.2	2.0	96.8	2.1	29.1	68.7	DC 3
1.4	2.5	96.1	5.3	29.4	65.4	DC 4
1.1	1.8	96.9	4.1	28.1	66.7	DC 5
4.2	2.0	93.8	11.6	22.1	66.3	DC 6
4.3	2.4	93.3	18.7	16.7	64.6	Alloy 1

(Ta)			Ta(Fe, Ni)			Remarks[a]
Fe	Ni	Ta	Fe	Ni	Ta	
7.0	3.0	90.0	28.7	13.8	57.5	Alloy 2
5.2	0.0	94.8	37.9	4.8	57.2	Alloy 3

Ta_2Ni			Ta(Fe, Ni)			Remarks[a]
Fe	Ni	Ta	Fe	Ni	Ta	
3.0	32.1	64.9	4.9	43.0	52.1	DC 1
2.7	31.5	65.8	7.4	43.0	51.6	DC 2
2.5	29.1	68.4	8.2	39.3	52.5	DC 3
5.9	29.7	64.4	10.8	37.1	52.1	DC 4
5.6	28.7	65.6	15.9	31.9	52.3	DC 5
12.1	23.3	64.5	31.2	1.7	52.1	DC 6

Ta(Fe, Ni)			$TaNi_2$			Remarks[a]
Fe	Ni	Ta	Fe	Ni	Ta	
6.0	45.3	48.7	1.4	64.9	33.7	DC 1
15.5	38.8	45.7	1.7	65.3	33.0	DC 2
17.5	37.0	45.5	12.5	53.1	34.4	DC 3

Ta(Fe, Ni)			Fe_2Ta			Remarks[a]
Fe	Ni	Ta	Fe	Ni	Ta	
19.4	33.4	47.3	35.7	28.6	35.7	DC 4
25.4	27.7	46.9	41.1	23.8	35.3	DC 5
35.9	17.0	47.1	55.2	10.2	34.5	DC 6
46.3	3.6	50.0	51.8	8.1	40.1	Alloy 5

$TaNi_2$			Fe_2Ta			Remarks[a]
Fe	Ni	Ta	Fe	Ni	Ta	
14.4	50.8	34.8	38.9	37.1	34.0	DC 3

$TaNi_2$			$TaNi_3$			Remarks[a]
Fe	Ni	Ta	Fe	Ni	Ta	
1.8	65.2	33.0	1.3	73.2	25.5	DC 1
1.6	65.7	32.7	2.2	72.3	25.5	DC 2

Fe_2Ta			$TaNi_3$			Remarks[a]
Fe	Ni	Ta	Fe	Ni	Ta	
28.0	39.7	32.3	4.4	70.4	25.2	DC 3

$TaNi_3$			(Fe, Ni)			Remarks[a]
Fe	Ni	Ta	Fe	Ni	Ta	
1.6	73.2	25.2	13.6	84.2	2.7	DC 1
3.4	72.4	24.2	21.8	75.7	2.5	DC 2
5.2	69.4	25.3	35.8	61.6	2.6	DC 3

Fe_2Ta			(Fe, Ni)			Remarks[a]
Fe	Ni	Ta	Fe	Ni	Ta	
46.7	24.5	28.8	48.1	50.4	1.4	DC 4
56.8	13.6	29.6	64.7	34.1	1.2	DC 5
65.3	5.0	29.7	84.1	15.4	0.5	DC 6

[a] The data from the diffusion couples and the ternary alloys are marked, where DC 1 ∼ 6 represent the six diffusion couples from $Fe_{12}Ni_{88}$/Ta to $Fe_{88}Ni_{12}$/Ta, respectively.

Table 4
The tie-triangle data on the phase equilibria of the Fe–Ni–Ta system at 1100 °C (in at.%).

Fe_2Ta			(Fe, Ni)			$TaNi_3$			Remarks[b]
Fe	Ni	Ta	Fe	Ni	Ta	Fe	Ni	Ta	
38.3	31.2	30.5	43.3	54.7	2.0	7.8	66.6	25.6	Alloy 6

$TaNi_2$			$TaNi_3$			Fe_2Ta			Remarks[b]
Fe	Ni	Ta	Fe	Ni	Ta	Fe	Ni	Ta	
10.4	55.7	33.9	3.2	71.0	25.8	–	–	–	Alloy 9

$TaNi_2$			Fe_2Ta			Ta(Fe, Ni)			Remarks[b]
Fe	Ni	Ta	Fe	Ni	Ta	Fe	Ni	Ta	
2.0	64.2	33.8	19.3	46.2	34.5	17.9	35.9	46.2	Alloy 10

[b] The data from the ternary alloys are marked.

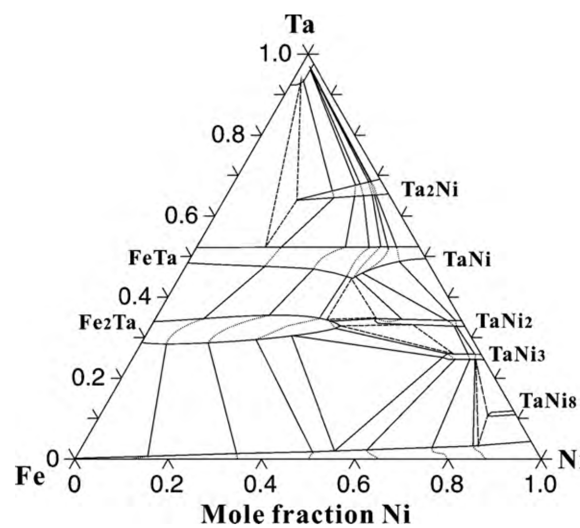

Fig. 5. Six diffusion paths according to the present work.

small in Alloy 9 (Fig. 2c), and only $TaNi_8$ was observed in Alloys 7 and 8.

According to the EPMA data at 1100 °C, the solubility of Fe in $TaNi_2$, and $TaNi_3$ was determined to be 18 and 7.8 at.%, respectively, while the solubility of Ni in Fe_2Ta was estimated to be 40 at.%. The solubility of Ta in phase (Fe, Ni) increased with the content of Ni, which agreed with the results obtained by Gupta [23] and Uskova [24]. The compounds FeTa and NiTa formed continuous solid solution.

Tables 3 and 4 listed the tie-line and tie-triangle data obtained with EDX/EPMA measurements of the diffusion couples and equilibrated alloys. Using these experimental data, the isothermal section at 1100 °C of the Fe–Ni–Ta system was constructed in Fig. 4. The six diffusion paths obtained from diffusion couples were given in Fig. 5. The measured phase relationships at 1100 °C in this work were agreement with the measured one at 1000 °C reported by Uskova [24]. Our measured phase relationships in the binary system agreed with the assessments [33–36].

4. Conclusions

The phase equilibria of the Fe–Ni–Ta system at 1100 °C were investigated using six (Fe–Ni alloy)/Ta diffusion couples, supplemented with ten equilibrated alloys. The experimental results showed no existence of ternary compounds at 1100 °C. The following five three-phase equilibria were obtained:

(1) (Ta) + Ta_2Ni + Ta(Fe, Ni), (2) Ta(Fe, Ni) + Fe_2Ta + $TaNi_2$, (3) Fe_2Ta + $TaNi_2$ + $TaNi_3$, (4) Fe_2Ta + $TaNi_3$ + (Fe, Ni), (5) $TaNi_3$ + $TaNi_8$ + (Fe, Ni). The compounds FeTa and NiTa formed continuous solid solution.

Acknowledgements

The financial support from the National Natural Science Foundation of China (50861006, 50971049), the Natural Science Foundation of Guangxi (0991002Z) and the Open Project Program of State Key Lab of Powder Metallurgy (2008112039) are greatly acknowledged.

References

[1] A.L. Greer, E. Ma, MRS Bull. 32 (2007) 611–619.
[2] C.F. Hsu, W. Kai, H.M. Lin, C.K. Lin, P.Y. Lee, J. Alloys Compd. (2010), doi:10.1016/j.jallcom.2010.02.061.
[3] J.W. Qiao, P. Feng, Y. Zhang, Q.M. Zhang, G.L. Chen, J. Alloys Compd. 486 (1/2) (2009) 527–531.
[4] K.A. Aly, A. Dahshan, F.M. Abdel-Rahim, J. Alloys Compd. 470 (1/2) (2009) 574–579.
[5] J.S.C. Jang, Y.S. Chang, T.H. Li, P.J. Hsieh, J.C. Huang, C.Y.A. Tsao, J. Alloys Compd. (2010), doi:10.1016/j.jallcom.2010.03.030.
[6] A.H. Cai, X. Xiong, Y. Liu, W.K. An, J.Y. Tan, Y. Pan, J. Alloys Compd. 468 (1/2) (2009) 432–437.
[7] Y.F. Sun, H. Fujii, N. Tsuji, Y. Todaka, M. Umemoto, J. Alloys Compd. 492 (1/2) (2010) 149–152.
[8] A.H. Cai, W.K. An, Y. Luo, T.L. Li, X.S. Li, X. Xiong, Y. Liu, J. Alloys Compd. 490 (1/2) (2010) 642–646.
[9] B.C. Lu, Y. Li, J. Xu, J. Alloys Compd. 467 (1/2) (2009) 261–267.
[10] B.C. Lu, Y. Li, J. Xu, J. Alloys Compd. 475 (1/2) (2009) 157–164.
[11] A.A. Elabbar, J. Alloys Compd. 476 (1/2) (2009) 125–129.
[12] J.L. Soubeyroux, S. Puech, J.J. Blandin, J. Alloys Compd. 483 (1/2) (2009) 107–111.
[13] C.Y. Tang, Y. Du, J. Wang, H.Y. Zhou, L.J. Zhang, F. Zheng, J. Lee, Q.R. Yao, Intermetallics 18 (5) (2010) 900–906.
[14] X.J. Liu, X.D. Hui, G.L. Chen, Intermetallics 16 (2008) 262–266.
[15] A. Makino, K. Mukasa, US Patent No. 4608228, August 26, 1986.
[16] H. Wada, R.D. Pehlke, Metall. Trans. B: Process Metall. 11 (1) (1980) 51–56.
[17] S.R. Reddy, R.G. Reddy, High Temp. Mater. Process. 23 (4) (2004) 261–290.
[18] R. Jayaganthan, J.P. Hajra, Scripta Mater. 37 (10) (1997) 1539–1544.
[19] J. Bourgeot, J. Manenc, Scripta Metall. 3 (8) (1967) 5770–6582.
[20] P. Rizzi, S. Barbero, L. Battezzati, Mater. Sci. Forum 360–362 (2001) 499–504.
[21] C.L. Zhu, Q. Wang, Y.M. Wang, J.B. Qiang, C. Dong, Intermetallics 18 (5) (2010) 791–795.
[22] L.I. Duarte, U.E. Klotz, C. Leinenbach, M. Palm, F. Stein, J.F. Löffler, Intermetallics 18 (3) (2010) 374–384.
[23] K.P. Gupta, Indian Inst. Met. 1 (1990) 316–320.
[24] E.N. Uskova, Mosc. Univ. Chem. Bull. (Engl. Transl.) 46 (1991) 81–84.
[25] H.H. Xu, Y. Du, Y.H. Tan, Y.H. He, S.T. Li, X. Zhang, J. Alloys Compd. 425 (1/2) (2006) 153–158.
[26] H.H. Xu, Y. Du, L.J. Zhang, S.T. Li, Z.P. Jin, J. Alloys Compd. 457 (1/2) (2008) 259–264.
[27] H.H. Xu, X. Xiong, Y. Du, P.S. Wang, B. Hu, Y.H. He, J. Alloys Compd. 485 (1/2) (2009) 249–254.
[28] W.W. Zhang, H.H. Xu, J.L. Liang, X. Wei, Y. Dong, J. Alloys Compd. 481 (2009) 509–514.
[29] A.A. Kodentsov, G.F. Bastin, F.J.J. van Loo, J. Alloys Compd. 320 (2003) 207–217.
[30] J.-C. Zhao, M.R. Jackson, L.A. Peluso, Acta Mater. 51 (2003) 6395–6405.
[31] L.J. Swartzendruber, E. Paul, J. Phase Equilib. 7 (3) (1986) 254–259.
[32] H. Okamoto, J. Phase Equilib. 17 (1) (1996) 81–82.
[33] S. Srikanth, A. Petric, J. Alloys Compd. 203 (1994) 281–288.
[34] I. Ansara, M. Selleby, CALPHAD 1 (1) (1994) 99–107.
[35] Y.W. Cui, Z.P. Jin, Z. Metallkd. 90 (3) (1999) 233–241.
[36] C. Servant, B. Sundman, O. Lyon, CALPHAD 25 (1) (2001) 79–95.